Characterization and Manipulation of the Acyl Chain Selectivity of Fatty Acid Amide Hydrolase†

Matthew P. Patricelli and Benjamin F. Cravatt*

The Department of Cell Biology and the Skaggs Institute for Chemical Biology, The Scripps Research Institute, 10550 North Torrey Pines Road, La Jolla, California 92037

Received November 8, 2000; Revised Manuscript Received February 16, 2001

ABSTRACT: Fatty acid amide hydrolase (FAAH) is a mammalian integral membrane enzyme that catabolizes several neuromodulatory fatty acid amides, including the endogenous cannabinoid anandamide and the sleep-inducing lipid oleamide. FAAH belongs to a large group of hydrolytic enzymes termed the amidase signature (AS) family that is defined by a conserved, linear AS sequence of approximately 130 amino acids. Members of the AS family display strikingly different substrate selectivities, yet the primary structural regions responsible for defining substrate recognition in these enzymes remain unknown. In this study, a series of unbranched *p*-nitroanilide (pNA) substrates ranging from 6 to 20 carbons in length was used to probe the acyl chain binding specificity of FAAH, revealing that this enzyme exhibits a strong preference for acyl chains 9 carbons in length or longer. A fluorophosphonate inhibitor of FAAH containing a photoactivatable benzophenone group was synthesized and used to locate a region of the enzyme implicated in substrate binding. Protease digestion and mass spectrometry analysis of FAAH−inhibitor conjugates identified the major site of cross-linking as residues 487−493. Site-directed mutagenesis revealed that a single residue in this region, I491, strongly influenced substrate specificity of FAAH. For example, an I491A mutant displayed a greatly reduced binding affinity for medium-chain pNA substrates (7−12 carbons) but maintained nearly wild-type binding and catalytic constants for longer chain substrates (14−20 carbons). Mutation of I491 to aromatic or more polar residues generated enzymes with relative hydrolytic efficiencies for medium- versus long-chain pNAs that varied up to 90-fold. Collectively, these studies indicate that I491 participates in hydrophobic binding interactions with medium-chain FAAH substrates. Additionally, the significant changes in substrate selectivity achieved by single amino acid changes suggest that FAAH possesses a rather malleable substrate binding domain and may serve, along with other AS enzymes, as a template for the engineering of amidases with novel and/or tailored specificities.

Fatty acid amide hydrolase (FAAH)[1] is a mammalian integral membrane enzyme responsible for the hydrolysis and inactivation of several members of the fatty acid amide family of signaling molecules (*1*−*6*). The most widely studied FAAH substrates are the endogenous cannabinoid anandamide (*N*-arachidonoyl ethanolamine) (*7*) and the sleep-inducing lipid oleamide (9-*Z*-octadecenamide) (*8*, *9*). Anandamide binds to and activates the central cannabinoid (CB1) receptor in vitro (*10*, *11*) and elicits cannabinoid-like pharmacological effects in vivo, including the induction of hypothermia, analgesia, hypomotility, and memory defects (*12*−*14*). Oleamide has been found to accumulate in the cerebrospinal fluid of sleep-deprived cats (*15*) and rats (*16*) and induces physiological sleep when administered to rats (*8*, *16*). The molecular site of action for the sleep effects of oleamide is currently unknown; however, this compound modulates the activity of several serotonergic receptors (*17*−*20*) and GABAergic receptors (*21*) in vitro. Numerous fatty acid amides in addition to oleamide and anandamide have been identified in mammals (*22*−*25*), suggesting that these compounds may represent a diverse family of biological signaling molecules.

FAAH is the only characterized mammalian member of a large class of enzymes termed the amidase signature (AS) family (*26*). All AS enzymes share a conserved, glycine-rich, linear AS sequence of approximately 130 amino acids. More than 80 known or predicted members of this family can be identified in public databases, including enzymes from archaea (*27*), eubacteria (*28*−*33*), fungi (*34*), nematodes, plants, insects, birds (*35*), and mammals (*1*). Recently, biochemical investigations of FAAH established that this enzyme is a nonclassical serine hydrolase that utilizes a Ser-Lys catalytic dyad instead of the more common Ser-His-Asp catalytic triad (*36*−*38*). All of the identified catalytic residues in FAAH are conserved among members of the AS family, indicating that these enzymes share a common catalytic mechanism (*38*).

† This work was supported by grants from the NIH (MH58542 and DA13173), the Skaggs Institute for Chemical Biology, the Searle Scholars Program (B.F.C.), and the National Science Foundation (M.P.P.).

* To whom correspondence should be addressed: e-mail cravatt@scripps.edu; phone 858-784-8633.

[1] Abbreviations: AS, amidase signature; ESI, electrospray ionization; FAAH, fatty acid amide hydrolase; FPBP, 4-(benzoylbenzyl)fluorophosphonic acid ethyl ester; HPLC, high-perfomance liquid chromatography; MALDI, matrix-assisted laser desorption ionization; MS, mass spectrometry.

10.1021/bi002578r CCC: $20.00
Published on Web 04/28/2001

Despite the high degree of primary structural homology shared by AS enzymes, their individual substrate selectivities vary widely. For example, members of the AS family have been found that preferentially hydrolyze fatty acid amides (*1*), acetamide (*34*), acrylamide (*31*), malonamide (*32*), nicotinamide (*30*), glutamine (*33*), indoleacetamide (*39*), and 6-aminohexanoate cyclic dimer (*40*). The molecular and structural features of AS enzymes that define substrate selectivity remain unknown, and no three-dimensional structure of an AS enzyme has yet been solved. Identifying the primary structural region(s) responsible for determining AS enzyme substrate selectivity is an important objective for at least two reasons. First, the characterization of essential substrate binding interactions for pharmaceutically relevant AS enzymes such as FAAH should facilitate the design of specific enzyme inhibitors and/or substrate analogues that might serve as important therapeutic agents and/or research tools. Second, manipulation of the substrate binding regions of AS enzymes may permit the creation of amidases with novel and/or tailored specificities, achieving a long-standing objective in the field of biocatalysis (*41*, *42*). With these two goals in mind, we have examined the substrate specificity of FAAH and, through photochemical cross-linking and site-directed mutagenesis, identified an isoleucine residue that strongly influences substrate recognition. The results of this study indicate that primary structural regions outside of the AS sequence contain at least part of the substrate binding domain of FAAH, and that single amino acid mutations in these regions can substantially alter substrate specificity.

EXPERIMENTAL PROCEDURES

General Methods. In all studies presented here, a transmembrane-domain-deleted form of FAAH containing a His_6 tag was expressed in *Escherichia coli* and purified as described (*43*). Deletion of the transmembrane domain has been shown to have no effect on the catalytic activity or membrane-binding properties of FAAH, yet it yields a more homogeneous preparation of enzyme when expressed in *E. coli* (*43*). Mutants were constructed by the Quickchange procedure (Stratagene). Regions of FAAH containing the desired mutations were subcloned into a wild-type (nonmutated) FAAH-pTrcHis vector by use of internal restriction sites and the entire subcloned region was sequenced to confirm that only the desired mutations were present. The panel of *p*-nitroanilide substrates was synthesized from the corresponding acid chlorides and 4-nitroaniline, with triethylamine as a base as described (*8*).

FAAH Activity Assays. The rates of FAAH-catalyzed hydrolysis of *p*-nitroanilide substrates were determined by monitoring the release of *p*-nitroaniline at 382 nm (ϵ = 13 500 M^{-1} cm^{-1}) on a Hewlett-Packard 8453 UV−visible spectrophotometer. Reactions were initiated by adding 20 μL of a 10× FAAH stock (in 20 mM Hepes, pH 7.8, 10% glycerol, 150 mM NaCl, and 1% Triton X-100) to 160 μL of reaction buffer (125 mM Tris, pH 9.0, and 1 mM EDTA), followed by the addition of 20 μL of 10× substrate in DMSO. The presence of 0.1% Triton X-100 and 10% DMSO greatly increased the solubility of the pNA substrates and did not hinder FAAH enzymatic activity. All K_m, k_{cat}, and k_{cat}/K_m values were determined in quadruplicate by Lineweaver−Burk plot analysis of at least four substrate concentrations. Errors represent the sample standard deviation of the quadruplicate measures.

Chemical Synthesis of 4-(Benzoylbenzyl)fluorophosphonic Acid Ethyl Ester (FPBP). FPBP was synthesized in four steps starting from commercially available 4-methylbenzophenone. Key intermediates in the synthesis were characterized by nuclear magnetic resonance (NMR) and matrix-assisted laser desorbtion ionization (MALDI) Fourier transform high-resolution mass spectrometry (FT-HRMS).

4-[(Bromomethyl)phenyl]phenylmethanone (**2**). A solution of 4-methylbenzophenone (**1**, 0.5 g, 2.55 mmol, 1.0 equiv), *N*-bromosuccinimide (0.544 g, 3.06 mmol, 1.2 equiv), and benzoyl peroxide (0.062 g, 0.26 mmol, 0.1 equiv) in $CHCl_3$ (10 mL) was refluxed for 1 h at 80 °C. The reaction was diluted with CH_2Cl_2 (100 mL) and washed sequentially with saturated aqueous NaH_2CO_3 (100 mL) and saturated aqueous NaCl (100 mL). The organic layer was dried (Na_2SO_4), and concentrated under reduced pressure to afford **2** (0.7 g, 0.7 g theoretical, 100%) as a white solid: ^{1}H NMR ($CDCl_3$, 250 MHz) δ 7.79−7.74 (m, 4H, arH), 7.57−7.54 (m, 1H, arH), 7.49−7.43 (m, 4H, arH), 4.50 (s, 2H, CH_2Br).

4-(Benzoylbenzyl)phosphonic Acid Diethyl Ester (**3**). A solution of 4-[(bromomethyl)phenyl]phenylmethanone (0.7 g, 2.55 mmol, 1.0 equiv) in triethyl phosphite (3 mL, 17.5 mmol, 6.9 equiv) was refluxed at 160 °C for 2 h. Excess triethyl phosphite was removed by vacuum distillation at 145 °C. Chromatography (SiO_2, 3 × 15 cm, 65% ethyl acetate/hexanes) afforded **3** (0.659 g, 0.846 g theoretical, 78%) as a yellow liquid: ^{1}H NMR ($CDCl_3$, 250 MHz) δ 7.77−7.72 (m, 4H, arH), 7.58−7.53 (m, 1H, arH), 7.48−7.37 (m, 4H, arH), 4.08−3.97 (m, 4H, CH_3CH_2O), 3.21 (d, J = 22.3 Hz, 2H, PCH_2Ar), 1.24 (t, J = 7.1 Hz, 6H, CH_3CH_2O); MALDI-FTMS (DHB) m/z 333.1256 ($C_{18}H_{21}O_4P + H^+$ requires 333.1256).

4-(Benzoylbenzyl)phosphonic Acid Monoethyl Ester (**4**). Bromotrimethylsilane (0.7 mL, 3.4 equiv) was added to a solution of 4-(benzoylbenzyl)phosphonic acid diethyl ester (0.510 g, 1.54 mmol, 1.0 equiv) in CH_2Cl_2 (15 mL) and the mixture was stirred for 30 min at 20 °C. The reaction was quenched with 5% aqueous $KHSO_4$ (15 mL), diluted with saturated aqueous NaCl, and extracted with CH_2Cl_2 (3 × 40 mL). The organic layers were dried (Na_2SO_4) and concentrated under reduced pressure. Chromatography (SiO_2, 3 × 15 cm, 15% CH_3OH/CH_2Cl_2 with 1% aqueous NH_4OH) afforded **4** (0.205 g, 0.468 g theoretical, 44%) as a white foam: ^{1}H NMR (CD_3OD, 250 MHz) δ 7.49−7.41 (m, 4H, arH), 7.35−7.31 (m, 1H, arH), 7.25−7.20 (m, 4H, arH), 3.68−3.55 (m, 2H, CH_3CH_2O), 2.86 (d, J = 22.1 Hz, 2H, PCH_2ar), 0.98 (t, J = 7.1 Hz, 3H, CH_3CH_2O); MALDI-FTMS (DHB) m/z 305.0940 ($C_{16}H_{17}O_4P + H^+$ requires 305.0937).

4-(Benzoylbenzyl)fluorophosphonic Acid Ethyl Ester (FPBP). A solution of 4-(benzoylbenzyl)phosphonic acid monoethyl ester (0.02 g, 0.07 mmol, 1.0 equiv) in CH_2Cl_2 (0.5 mL) at −78 °C was treated with (diethylamino)sulfur trifluoride (DAST, 0.018 mL, 0.14 mmol, 2 equiv) and stirred for 5 min. Solvent was removed under a stream of N_2 gas and the products were chromatographed (SiO_2, 0.5 × 4 cm, 50% ethyl acetate/hexanes) to yield FPBP (0.0141 g, 0.021 g theoretical, 70%) as a clear oil: ^{1}H NMR ($CDCl_3$, 250 MHz) δ 7.79−7.75 (m, 4H, arH), 7.62−7.60 (m, 1H, arH), 4.28−4.16 (m, 2H, CH_3CH_2O), 3.37 (dd, J = 23.2 Hz/2.6 Hz, 2H,

PCH_2ar), 1.30 (t, J = 7.1 Hz, 3H, CH_3CH$_2$O); MALDI-FTMS (DHB) m/z 329.0726 ($C_{16}H_{16}O_3PF + Na^+$ requires 329.0713)

Cross-Linking of FAAH with FPBP. In a typical experiment, FAAH (1−2 mg/mL, 15−30 μM) was treated with 50 μM FPBP and incubated in the dark for 30 min in an eppendorf tube. The cross-linker was then activated by exposure to a hand-held UV lamp (15 W) at 365 nm for 30 min. Control reactions included (1) FAAH that was not treated with FPBP and was exposed to the UV light and (2) FAAH that was treated with FPBP and kept in the dark.

Identification of the Site of FPBP Cross-Linking to FAAH. The UV-irradiated FAAH sample and appropriate controls were denatured by the addition of solid urea to 8 M. The samples were then heated to 65 °C for 10 min. Reduction/alkylation was performed by treating the samples with 2 mM DTT for 30 min at 37 °C, followed by 5 mM iodoacetamide for 30 min at 37 °C. The samples were then diluted 4-fold with 50 mM ammonium bicarbonate and treated with 1−5 μg trypsin (sequencing-grade modified trypsin, Promega) per 100 μg of FAAH for 12 h at 37 °C. Peptides resulting from the tryptic digest were separated by HPLC on an analytical C4 reverse-phase column (Higgins Analytical) equilibrated in 98.5% buffer A (H_2O, 0.1% trifluoroacetic acid) and 1.5% buffer B (CH_3CN, 0.08% trifluoroactetic acid). The peptides were eluted with the following gradient: 0−60 min (1.5−30% buffer B), 60−120 min (30−60% buffer B). Peaks of interest were collected manually and concentrated under reduced pressure. The purified and concentrated FPBP cross-linked peptide adduct obtained from 200 μg of digested FAAH protein was resuspended in 10 μL of 50% CH_3CN and then diluted 5-fold with 100 mM Tris, pH 8.0. Chymotrypsin (1 μg, sequencing-grade chymotrypsin, Boehringer Mannheim) was added and the peptide adduct digested for 2 h at 37 °C. The resulting digest was analyzed by MALDI mass spectrometry on a PerSeptive Biosystems Voyager-DE to identify the site of cross-linking. Samples from the crude digests were prepared for MALDI analysis with Zip Tips (Millipore) to remove salts and buffers according to the manufacturer's instructions.

RESULTS

Substrate Specificity of FAAH. The binding and catalytic specificities of FAAH were determined for various unbranched *p*-nitroanilide (pNA) substrates bearing acyl chains 6−20 carbons in length (Table 1). The use of pNA substrates allowed for the precise monitoring of enzymatic hydrolysis rates by following the increase in UV absorbance at 382 nm due to the release of *p*-nitroaniline. We have previously found that pNAs are slower FAAH substrates than the corresponding primary amides; however, the binding affinities of these two classes of substrates were equivalent (*37*). Due to the slower rates of pNA hydrolysis relative to the corresponding primary amides, it can be assumed that pNA substrates are hydrolyzed by FAAH in an acylation rate-limiting manner, allowing for the direct measurement of substrate binding constants through the determination of K_m values ($K_m = K_s$).

A clear pattern of substrate selectivity was observed with the pNA substrates listed in Table 1. The k_{cat} values of the substrates tested varied less than 3-fold while the K_m values dropped sharply from >2 mM for hexanoyl pNA to 74 μM for nonanoyl pNA. The catalytic efficiency (k_{cat}/K_m) of FAAH for nonanoyl pNA was approximately 50-fold higher than for hexanoyl pNA, a change that can be attributed mainly to a gain in substrate binding affinity. The K_m values for substrates bearing acyl chains 9−20 carbons in length were essentially constant. The k_{cat} values for 14−20 carbon pNAs were slightly (2-fold) lower than those of the 9−12 carbon pNAs, making the latter class more efficient substrates. Overall, the catalytic properties displayed by FAAH for the panel of pNA substrates tested indicate that relatively strong enzyme−substrate binding interactions occur between the 6th and 9th carbons of the pNA acyl chain.

Table 1: Substrate Selectivity of FAAH

substrate	k_{cat} (s^{-1})	K_m (μM)	k_{cat}/K_m (M^{-1} s^{-1})
hexanoyl pNA	≥0.38	≥2000	170 ± 10
heptanoyl pNA	0.46 ± 0.02	410 ± 20	1120 ± 50
octanoyl pNA	0.73 ± 0.07	220 ± 30	3320 ± 170
nonanoyl pNA	0.60 ± 0.04	74 ± 10	8100 ± 700
decanoyl pNA	0.56 ± 0.03	57 ± 2	9800 ± 200
lauroyl (C12) pNA	0.46 ± 0.03	65 ± 6	7100 ± 300
myristoyl (C14) pNA	0.29 ± 0.02	99 ± 14	2900 ± 200
palmitoyl (C16) pNA	0.27 ± 0.03	74 ± 7	3600 ± 100
oleoyl (C18) pNA[a]	0.27 ± 0.02	74 ± 8	3600 ± 200
arachidonoyl (C20) pNA[a]	0.48 ± 0.05	60 ± 8	8000 ± 200

[a] Saturated pNA substrates with >16 carbon acyl chains could not be used due to their low solubility. The unsaturated substrates oleoyl (9-*Z*-octadecenoyl) pNA and arachidonoyl (5,7,9,11-*Z*-eicosatetraenoyl) pNA were used due to their increased solubility and similarity to proposed biological substrates of FAAH.

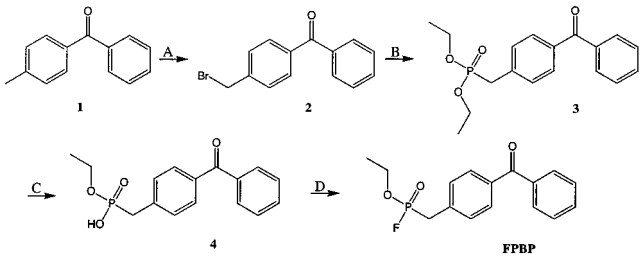

FIGURE 1: Synthesis of 4-(benzoylbenzyl)fluorophosphonic acid ethyl ester (FPBP). 4-Methyl benzophenone (**1**) was converted to FPBP (**4**) in four steps as detailed: (A) benzoyl peroxide, NBS, Δ; (B) $P(OEt)_3$, Δ; (C) TMSBr; (D) DAST.

Identification of a Substrate Binding Site in FAAH. To identify the region(s) of FAAH responsible for substrate binding, inhibitors were synthesized that possess photoactivatable cross-linking groups. This general strategy took advantage of the potent, irreversible inhibition of FAAH by fluorophosphonates (*36*, *44*). Several photoactivatable cross-linkers were synthesized that contain a fluorophosphonate group coupled to either perfluorophenyl azide (*45*) or benzophenone groups through linkers of varied lengths (not shown). While all of the agents were capable of irreversibly inhibiting FAAH, only the benzophenone-containing inhibitor FPBP (Figure 1) resulted in efficient cross-linking to a specific position in FAAH. The distance between the photoreactive carbonyl of FPBP and its electrophilic phosphate atom was approximately equivalent to 6−7 carbons of an extended alkyl chain.

The reaction of FPBP with the nucleophile of FAAH was confirmed by the identification of a 2958 Da peptide in tryptic digests of an FPBP-treated FAAH sample. This peptide matched the expected mass of a tryptic peptide

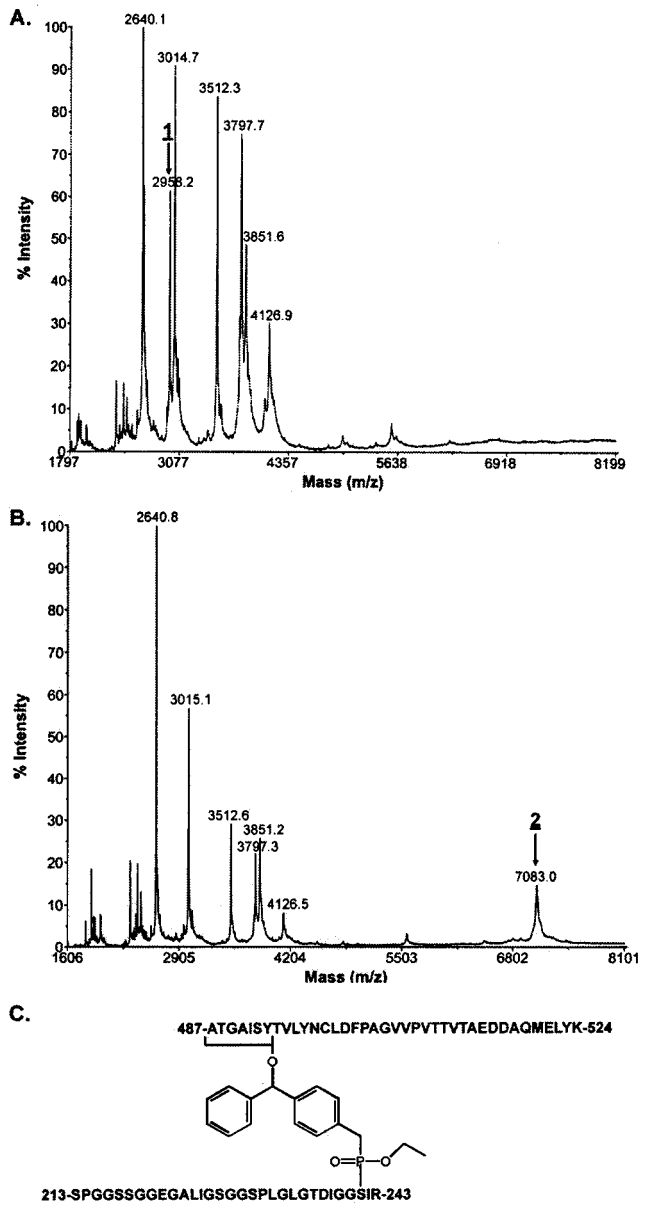

FIGURE 2: MALDI-MS analysis of FPBP-cross-linked FAAH. FAAH was treated with FPBP and either exposed to UV light for 30 min (B) or kept in the dark (A) prior to digestion with trypsin. MALDI-MS of the resulting peptides revealed the presence of a novel peak in the UV-activated sample with a mass of 7083 Da. This mass corresponds to an FPBP-cross-linked adduct between a peptide containing the nucleophile of FAAH (S241) and a peptide spanning residues 487−524 (C).

(residues 213−243) containing the serine nucleophile of FAAH (S241) reacted with one molecule of FPBP (Figure 2A). The MALDI-MS profile of tryptic digests from FAAH samples treated with FPBP and activated with UV light revealed the presence of a novel peak with a mass of 7083 Da (Figure 2B). This peptide matched the expected mass of an adduct between two FAAH tryptic peptides, residues 213−243 and 487−524, cross-linked by one molecule of FPBP (Figure 2C).

Reverse-phase HPLC profiles of tryptic digests obtained from UV-activated samples of FPBP-treated and untreated FAAH confirmed the presence of a cross-linked adduct resulting from the UV activation of FPBP (Figure 3A). As expected, the peptide corresponding to residues 213−243

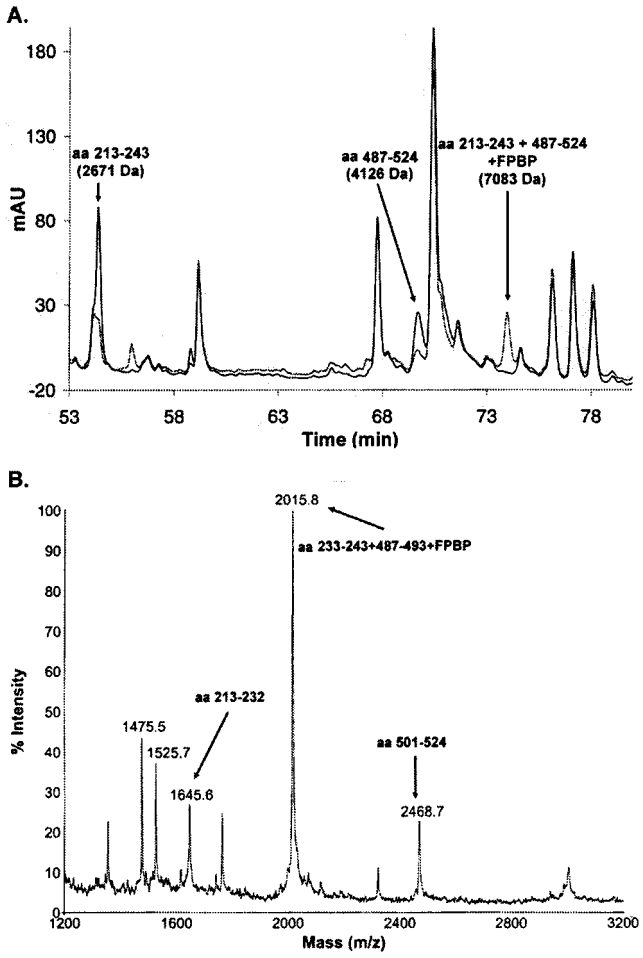

FIGURE 3: Identification of the site of FPBP cross-linking in FAAH. (A) The HPLC profiles of tryptic peptides from a FAAH sample treated with FPBP and exposed to UV light (gray trace) and an untreated FAAH control (black trace) are shown. In the FPBP-treated sample, two peptides (containing residues 213−243 and 487−524) were significantly depleted, while a novel peak corresponding to the FPBP-cross-linked adduct of these two peptides was observed eluting at 74 min. This adduct was isolated, digested with chymotrypsin, and analyzed by MALDI-MS (B). A major peak with *m*/*z* 2015.8 was observed that matched the expected mass of residues 233−243 and 487−493 linked by one molecule of FPBP.

was greatly reduced in the FPBP-treated sample, as was a second peak containing a peptide with a mass of 4126 Da, corresponding to residues 487−524. A novel peak was observed in the UV-cross-linked peptide profile at 74 min that contained two peptides with masses of 7083 and 6807 Da. The former mass matched the mass observed previously in the MALDI profile of tryptic digests of a photoactivated FAAH−FPBP sample (corresponding to an FPBP cross-linked adduct of two tryptic peptides containing residues 213−243 and 487−524, respectively). The latter adduct corresponded to the product of a photo-cross-link between the nucleophile-containing peptide (213−243) and a peptide representing residues 176−209. The un-cross-linked 176−209 peptide eluted at 70 min, along with two other peptides, and the decrease in this peak upon UV treatment was not consistently significant.

Although attempts to separate the two species of cross-linked peptides by HPLC were unsuccessful, the peak corresponding to the 487−524 peptide was consistently decreased more than 70% in FPBP-cross-linked samples

Table 2: Catalytic Properties of FAAH Mutants

	nonanoyl pNA			myristoyl pNA			oleoyl pNA		
	k_{cat} (s^{-1})	K_m (μM)	k_{cat}/K_m (M^{-1} s^{-1})	k_{cat} (s^{-1})	K_m (μM)	k_{cat}/K_m (M^{-1} s^{-1})	k_{cat} (s^{-1})	K_m (μM)	k_{cat}/K_m (M^{-1} s^{-1})
FAAH	0.60[a]	74	8100	0.29	99	2900	0.27	74	3600
A487V	0.60	57	10500	0.13	69	1900	0.21	83	2500
T488A	0.51	179	2850	0.19	92	2060	0.21	95	2210
G489A	0.20	73	2700	0.14	94	1500	0.25	98	2550
I491A	0.58	570	1000	0.21	72	2900	0.22	126	1700

[a] Values represent the mean of four independent measurements. The standard deviations of the kinetic parameters were k_{cat} < 10%, K_m < 15%, and k_{cat}/K_m < 10%.

relative to un-cross-linked controls. Since each nucleophile-bound cross-linker can only react to form one adduct, the species containing residues 487−524 (resulting in an adduct with a mass of 7083 Da) likely constituted the major cross-linked product. In support of this notion, the HPLC peak at 74 min exhibited a UV spectrum consistent with the presence of tyrosine but not tryptophan residues (not shown). The 487−524 peptide contains three tyrosine residues, while the 176−209 peptide lacks tyrosines but contains one tryptophan residue. Given the much higher extinction coefficient of tryptophan relative to tyrosine, it is likely that the major species present in the 74 min HPLC peak was the cross-linked adduct containing the 487−524 peptide.

Considering that the peptides cross-linked by FPBP represented the two largest FAAH tryptic peptides, together covering 70 residues, tandem MS analysis was conducted in attempts to refine the sites of photo-cross-linking. These experiments were mostly unsuccessful due to both the large sizes of the two peptide adducts and the apparent fragmentation of the bond formed by the activated cross-linker. Nonetheless, the fragmentation patterns obtained in the tandem MS experiments confirmed the identities of the peptides cross-linked by FPBP as those containing residues 487−524 (mass of 7083 Da) and 176−209 (mass of 6807 Da).

Further digestion of the HPLC-purified FPBP peptide adducts with chymotrypsin yielded several peptides resulting from cleavage of the 7083 Da cross-linked adduct, including a peptide with a mass of 2015.8 Da (Figure 3B). This fragment has the expected mass of a chymotrypsin-cleaved fragment containing the catalytic nucleophile (residues 233−243) attached to residues 487−493 through one molecule of FPBP. Additional peaks were observed in the MALDI spectrum at 1645.6 and 2468.7 Da, corresponding to fragments containing the unmodified residues 213−232 and 501−524, respectively. Peptides resulting from cleavage of the 6807 Da cross-linked species were not observed following digestion with chymotrypsin, likely due to the low original signal of this adduct. These results indicate that the major site of cross-linking for FPBP lies within residues 487−493 of FAAH.

Site-Directed Mutagenesis of FAAH Residues 487−493. With the major site of FPBP cross-linking restricted to a seven-residue sequence of FAAH (487−493), the potential role that this region plays in substrate recognition was examined by site-directed mutagenesis. Seven mutants were originally constructed: A487V, T488A, G489A, A490V, I491A, S492A, and Y493A. Three of these mutants, A490V, S492A, and Y493A, resulted in proteins that were expressed only in inclusion bodies and no active protein could be recovered from *E. coli* lysates. Further mutation of Y493 to either L or W also failed to produce active, soluble proteins.

Four mutants, A487V, T488A, G489A, and I491A, expressed to levels comparable to those of wild-type FAAH, and their kinetic parameters with nonanoyl, myristoyl, and oleoyl pNA substrates were determined (Table 2). These mutation had relatively minor effects on the K_m (≤1.7-fold), k_{cat} (≤2.2-fold), and k_{cat}/K_m (≤2.1-fold) values for the myristoyl and oleoyl pNA substrates. Two mutants, T488A and I491A, exhibited significantly higher K_m values for nonanoyl pNA while retaining wild-type k_{cat} values for this substrate. The K_m value for I491A-catalyzed hydrolysis of nonanoyl pNA (570 μM) was nearly 8-fold higher than the wild-type K_m value for this substrate (74 μM). In contrast, the I491A mutant exhibited a K_m value for myristoyl pNA (72 μM) that was slightly lower than the wild-type value (99 μM). The increase in the K_m value for nonanoyl pNA displayed by the I491A mutant, in conjunction with the nearly wild-type k_{cat} values exhibited by this enzyme, are consistent with a role for I491 in discrete substrate binding events.

The catalytic properties of the I491A mutant were determined with a broader panel of pNAs to examine the precise effects of this mutation on substrate recognition (Figure 5). The k_{cat}/K_m values for I491A-mediated hydrolysis of saturated pNAs deviated most strongly from wild-type values with substrates bearing acyl chains 7−12 carbons in length. For example, hexanoyl pNA and myristoyl pNA were each hydrolyzed by the I491A mutant and FAAH with nearly equivalent catalytic efficiencies (k_{cat}/K_m), while decanoyl pNA was hydrolyzed by the I491A mutant with 12-fold lower efficiency. Interestingly, for the most affected substrates, nonanoyl and decanoyl pNA, increases in K_m values for the I491A mutant accounted for nearly all of the observed decreases in k_{cat}/K_m.

Although the catalytic properties of the I491A mutant were consistent with I491 participating directly in substrate binding, the loss of binding affinity upon mutation of this residue could also have originated from indirect effects on neighboring residues. To further test whether I491 represents a residue directly involved in substrate binding, the efficiency of FPBP cross-linking was determined for the I491A mutant. When the I491A mutant was incubated with FPBP and treated with UV light, no evidence of cross-linked species was observed by HPLC electrospray ionization MS (HPLC-ESI-MS) (Figure 4) or MALDI-MS (not shown). Additionally, the peak height of the tryptic peptide corresponding to residues 487−524 (4083 Da) remained constant after photoactivation, indicating that little or no cross-linking of this peptide to the FPBP-bound 213−243 peptide had occurred.

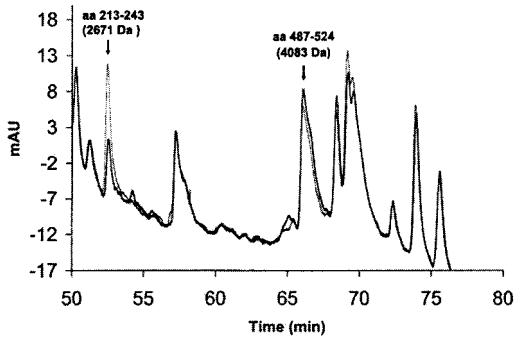

FIGURE 4: Absence of detectable FPBP cross-linking for the I491A mutant. The HPLC profiles of tryptic peptides from a sample of the I491A mutant treated with FPBP and exposed to UV light (black trace) and an untreated I491A mutant control (gray trace) are shown. Reaction of FPBP with the nucleophile of the mutant enzyme (S241) was confirmed by the decrease in a peak at 52 min containing a peptide with the mass of 2671 Da, corresponding to aa 213−243. The peptide containing alanine 491 (aa 487−524; 4126 Da) coeluted at 66 min with a peptide containing residues 541−563 (2640 Da). No evidence of FPBP-mediated cross-linking was observed, as judged by (1) the lack of decrease in the height of the UV peak at 66 min, (2) the absence of any new peptide peaks detectable by UV absorbance, and (3) the lack of detection by ESI-MS analysis of a peptide with the mass of 7041 Da (the predicted mass for residues 213−243 and 487−524 of the I491A mutant cross-linked by one molecule of FPBP).

As an additional control, wild-type FAAH was mixed with the I491A mutant at a 1:10 ratio, treated with FPBP, UV-cross-linked, and analyzed by HPLC-ESI-MS. In this experiment, the cross-linked adduct between the 213−243 and 487−524 peptides was readily detected for wild-type FAAH by both UV absorbance and ESI-MS, but no such adduct could be found for the I491A mutant enzyme (data not shown). These data support that I491 participates in the binding of FPBP at or near its photoreactive carbonyl and, when combined with the substrate selectivity results described above for the I491A mutant, suggest further that this residue plays a direct role in substrate recognition.

Modifying the Substrate Selectivity of FAAH by Mutation of I491. The substantial changes in substrate selectivity observed upon mutation of I491 to alanine suggested that this residue in FAAH was of central importance for substrate recognition. To further explore the impact of residue 491 on the substrate selectivity of FAAH, several mutants bearing different amino acids at position 491 were generated and tested for their relative hydrolytic efficiencies with representative pNA substrates (Table 3, Figure 6). Mutation of I491 to a residue with a more polar side chain, I491Y, generated a FAAH variant exhibiting a substrate selectivity similar to that of the I491A mutant (decreased catalytic efficiency with nonanoyl pNA relative to myristoyl and oleoyl pNA). In contrast, an I491F mutant hydrolyzed nonanoyl pNA with significantly higher catalytic efficiency than myristoyl or oleoyl pNA. The I491Y and I491F mutants exhibited nearly identical catalytic efficiencies with long-chain pNAs (reduced 3−5-fold relative to FAAH). Interestingly, an I491W mutant was found to hydrolyze nonanoyl pNA at least 15-fold more efficiently than oleoyl pNA or myristoyl pNA. In contrast to the results obtained with the I491A mutant, the relative changes in substrate selectivity observed for the I491Y, I491F, and I491W mutants originated from changes in k_{cat} as well as K_m values for the three substrates (Table 3). In summary, substitutions of appropriately sized hydrophobic residues, I, F, or W, at the 491 position favored the hydrolysis of nonanoyl pNA, while placement of a small (alanine) or polar (tyrosine) residue at this position resulted in enzymes that preferred longer chain pNAs. In the most extreme case, these single-site mutations led to the production of enzymes exhibiting up to 90-fold differences in their respective ratios of medium/long-chain pNA catalytic efficiencies (k_{cat}/K_m).

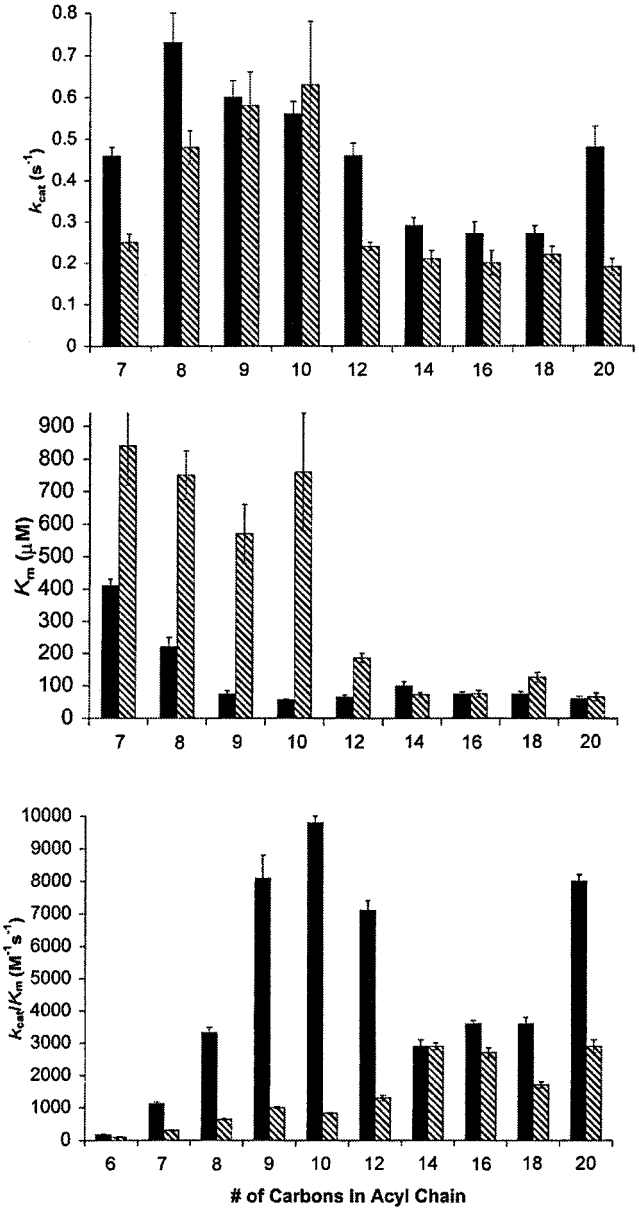

FIGURE 5: Kinetic analysis of the I491A mutant. Shown are the k_{cat} (upper panel), K_m (middle panel), and k_{cat}/K_m (lower panel) values measured for FAAH (black) and an I491A mutant (black hatched) with pNA substrates containing acyl chains of the indicated number of carbons. Large increases in K_m and decreases in k_{cat}/K_m were observed for the I491A mutant for substrates with acyl chains bearing 7−12 carbons.

DISCUSSION

The substrate selectivity of FAAH has been described as "nonselective", on the basis of the observation that this enzyme hydrolyzes a variety of long-chain fatty acid amides.

Table 3: Catalytic Properties of I491 Mutants

	nonanoyl pNA			myristoyl pNA			oleoyl pNA		
	k_{cat} (s^{-1})	K_m (μM)	k_{cat}/K_m (M^{-1} s^{-1})	k_{cat} (s^{-1})	K_m (μM)	k_{cat}/K_m (M^{-1} s^{-1})	k_{cat} (s^{-1})	K_m (μM)	k_{cat}/K_m (M^{-1} s^{-1})
FAAH	0.60[a]	74	8100	0.29	99	2900	0.27	74	3600
I491W	0.56	152	3670	0.035	145	240	0.026	129	200
I491F	0.34	182	1870	0.096	90	1070	0.070	100	700
I491A	0.58	570	1000	0.21	72	2900	0.22	126	1700
I491Y	0.051	355	140	0.062	76	820	0.065	114	570

[a] Values represent the mean of four independent measurements. The standard deviations of the kinetic parameters were k_{cat} < 10%, K_m < 15%, and k_{cat}/K_m < 10%.

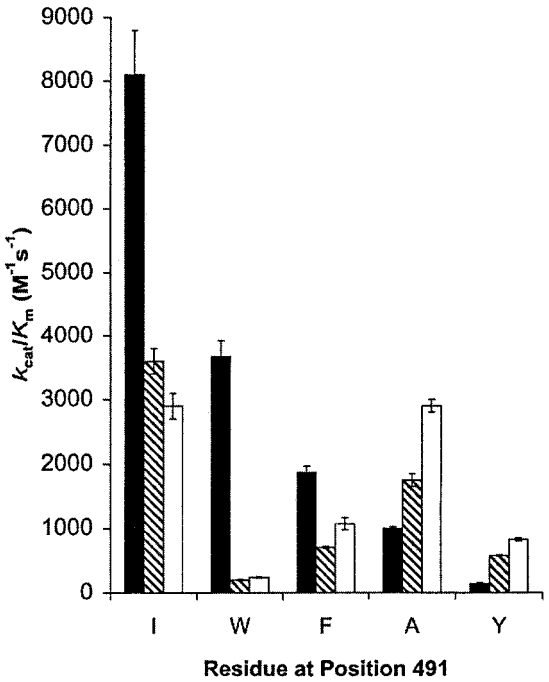

FIGURE 6: Relative catalytic efficiencies of various I491 mutants. I491 was substituted with W, F, A, and Y and the k_{cat}/K_m values for nonanoyl (black), oleoyl (black hatched), and myristoyl (white) pNA hydrolysis were measured. In general, the presence of hydrophobic residues at position 491 favored medium-chain (nonanoyl) pNA hydrolysis, while polar or small residue substitutions resulted in enzymes that hydrolyzed long-chain (myristoyl and oleoyl) pNAs with higher efficiency.

Studies of leaving group selectivity have revealed that FAAH can accept as substrates both primary amides and secondary amides with numerous substitutions, including aromatic rings and oxygenated and branched alkyl substituents (*46*). Further, a variety of long-chain (>12 carbons) fatty acid amide and ethanolamide substrates with varied degrees and positions of unsaturation were found to be efficient FAAH substrates (*4*, *46*). Although the aforementioned observations indicate that the substrate requirements of FAAH are relatively flexible, the studies presented here reveal that the enzyme exhibits significant selectivity for substrates with acyl chains longer than eight carbons. It is interesting to note that the preference that FAAH displays for long-chain fatty acid amides is consistent with its proposed role as the primary catabolic route for these signaling lipids in vivo (*1*, *47*).

The substrate selectivity of FAAH with a panel of pNAs was found to match closely results from two previous studies that used trifluoromethyl ketone (*48*) and α-keto heterocycle (*49*) inhibitors to probe the acyl chain specificity of the enzyme. It is important to note, however, that the electrophilic carbonyl-based inhibitors employed in these studies form covalent, reversible enzyme−inhibitor adducts with FAAH. The factors that influence binding of such inhibitors likely involve a combination of noncovalent interactions with the acyl chain of the inhibitor, proper positioning and reactivity of its electrophilic carbonyl, and the stability of the resulting covalent adduct. The latter set of factors could correlate with substrate K_m and/or k_{cat} values or may be inhibitor-specific and therefore not predictive of substrate behavior. The binding of FAAH inhibitors was found to depend strongly on the first 8−9 carbons of the acyl chain, with K_i values decreasing 3−10-fold for each additional carbon up to the ninth position. Inhibitors with 14−16 carbon acyl chains had somewhat reduced potency (3−4-fold) relative to 9−12 carbon inhibitors, while compounds with >16 saturated carbons were significantly less potent (10−20-fold). Unsaturated inhibitors with >16 carbons exhibited potencies similar to those of agents with 14−16 carbons. This structure−activity relationship for FAAH inhibitors is essentially identical to the k_{cat}/K_m profile that the enzyme displayed for the panel of pNA substrates examined herein, with the exception that very long chain (>16 carbon) saturated pNAs were not tested in this study. Interestingly, the increases in k_{cat}/K_m observed while progressing from hexanoyl pNA to nonanoyl pNA were due almost entirely to binding effects (K_m), while the decreased relative catalytic efficiencies of 14−20 carbon substrates resulted from changes in k_{cat} values. Thus, increases in inhibitor potency due to variations in acyl chain length were predictive of both the substrate binding (K_m) and catalytic (k_{cat}) preferences of FAAH. In summary, the relative potency of electrophilic FAAH inhibitors correlated well with the overall substrate selectivity (k_{cat}/K_m) profile of the enzyme.

To identify the region(s) of FAAH responsible for substrate/inhibitor binding, an irreversible inhibitor−photoactivatable cross-linker (IIPC) was synthesized that possesses a nucleophile-directed fluorophosphonate and a photoreactive benzophenone (FPBP). The latter moiety was positioned near the predicted location of the 6th or 7th carbon of an extended fatty acid amide substrate. Typically, reversible inhibitors/binding groups are used in photo-cross-linking experiments (*50*), possibly due to the greater availability of reversible probes for most proteins. The use of an IIPC in this study offered several important advantages for photoreactive cross-linking. First, FPBP alleviated the need to obtain a tight-binding reversible FAAH inhibitor that maintained its high binding affinity after incorporation of a somewhat bulky photo-cross-linking moiety. Second, the cross-linking yields of reversibly bound photoreactive cross-linkers depend to a large extent on the off rates of these agents; a value too high

relative to the rate of photoreaction can result in low efficiencies of specific cross-linked adduct and/or significant nonselective cross-linking. Off rates do not apply to IIPCs, as these agents are stably bound to the active site. Thus FPBP was well suited to provide maximal cross-linking efficiency to the substrate binding pocket of FAAH. Third, the light-induced reaction of an IIPC results in the covalent coupling of an active-site amino acid to the site of cross-linking. This feature allowed for the unambiguous identification of cross-linking reactions that occurred while FPBP was bound in the active site of FAAH. Importantly, the use of an IIPC could conceivably be extended to identify interactions between proteins in a complex or between an enzyme active site and molecules in the surrounding microenvironment (i.e., lipids, DNA, RNA, carbohydrates). Finally, it is noteworthy that the fluorophosphonate reactive group used in FPBP reacts with nearly all serine hydrolases including proteases, lipases, and esterases, and thus FPBP and/or related fluorophosphonate-based IIPCs could prove broadly applicable to the structural analysis of this large enzyme superfamily.

The major site of photoinduced FPBP cross-linking in FAAH was found to reside in the tryptic peptide bearing residues 487−524. Based on the observed decrease in the HPLC peak corresponding to this peptide upon photoactivation, the efficiency of cross-linking of FPBP to the 487−524 peptide was estimated to be ~70%. A second adduct was also observed with FAAH residues 176−209, which appeared to account for a much lower fraction of cross-linking events. Due to the high efficiency of cross-linking, sufficient quantities of the cross-linked product could be purified from trypsin digests for further protease digestion steps and analysis by tandem mass spectrometry without necessitating the use of a radiolabel. These efforts identified a relatively confined region of FAAH encompassing residues 487−493 as the major site of cross-linking. Interestingly, this region is highly conserved among the mammalian FAAH enzymes (*2*) but shares little sequence similarity with the corresponding segments of other AS enzymes. On the basis of the widely varied substrate selectivities displayed by members of the AS family, it might not be surprising if their substrate binding domains represent less conserved regions of their primary structures (i.e., regions other than the AS sequence).

Site-directed mutagenesis of FAAH residues within the major region of photo-cross-linking (487−493) identified I491 as a possible site for photoreaction with FPBP and a strong candidate for direct participation in substrate binding interactions. Removal of this potential binding residue by mutation of I491 to alanine diminished the binding affinity of FAAH for medium-chain (7−12 carbon) substrates up to 13-fold but had no effect on the binding of long-chain substrates. Substitution of I491 with a more polar tyrosine residue also resulted in an enzyme with reduced relative catalytic efficiency for medium-chain pNAs, while a phenylalanine substitution at this site produced an enzyme with a substrate specificity similar to that of wild-type FAAH. Interestingly, the I491Y and I491F mutants shared nearly identical k_{cat}/K_m values for oleoyl and myristoyl pNA, while the efficiency of nonanoyl pNA catalysis was more than 13-fold lower for the I491Y mutant, suggesting that the hydroxyl group of tyrosine 491 was responsible for the decrease in nonanoyl pNA hydrolysis efficiency. Substitution of I491 with another hydrophobic residue, tryptophan, also resulted in an enzyme that hydrolyzed nonanoyl pNA with greater efficiency than oleoyl or myristoyl pNA. These observations suggest that I491 is responsible for direct hydrophobic binding interactions with FAAH substrates bearing acyl chains 7−12 carbons in length.

In contrast to the effects of the I491A mutation, which impacted primarily K_m values, the altered substrate selectivities of the I491Y, I491F, and I491W mutants resulted from changes in both k_{cat} and K_m values. In all cases, however, the relative magnitude of k_{cat} changes was different for medium- and long-chain substrates. This differential k_{cat} effect could be most clearly visualized in pairwise comparisons of either FAAH and the I491A mutant or of the I491F mutant and the I491Y mutant. In both cases, the absolute efficiency of myristoyl pNA hydrolysis was similar for the two enzymes under comparison, but nonanoyl pNA hydrolytic efficiencies were substantially different. Although it is not clear why mutations in I491 would in certain cases cause selective k_{cat} effects, this behavior is not inconsistent with I491 making substrate contacts in the active site of FAAH. Indeed, similar mixed k_{cat} and K_m effects have been observed following mutation of substrate binding residues in the active site of subtilisin (*51*, *52*) and trypsin (*53*).

The substantial differences in the behavior of medium- (7−12 carbon) and long-chain (14−20 carbon) substrates with the I491 mutants is surprising considering the absence of binding discrimination by the wild-type enzyme for these two substrate classes. The K_m (or K_i) values of FAAH substrates (or inhibitors) are remarkably constant for compounds bearing acyl chains of nine or more carbons, initially suggesting that FAAH might not interact with substrates or inhibitors beyond the ninth carbon of the acyl chain. However, for the I491A mutant, K_m values for substrates with 7−10 carbons were essentially constant but then decreased significantly as the acyl chain grew to 12−14 carbons (see Figure 5). This behavior could be interpreted as evidence for a binding interaction taking place in the I491A mutant that is absent in FAAH. However, an alternative possibility is that the binding contacts made by medium- and long-chain pNAs are at least partially nonoverlapping. It is conceivable that such binding subtleties would be necessary to avoid nonproductive binding modes for longer chain FAAH substrates. For example, a simple, relatively short hydrophobic binding pocket might allow long-chain FAAH substrates to occupy the hydrophobic binding site in several configurations with equivalent affinities, most of which might place the amide carbonyl out of register for nucleophilic attack. Regardless, these data highlight that the chemical and biochemical approaches utilized herein offer insights into the functional properties of FAAH in solution that might be difficult to predict from static images obtained through three-dimensional structure determinations of the enzyme.

In summary, the hydrolysis of amides is one of the more difficult and important reactions encountered in both biological and chemical systems (*41*, *42*). In the course of these studies, several amidase enzymes were generated that exhibited significantly different substrate selectivities for various straight-chain alkyl amides. In the most extreme example, the nonanoyl/myristoyl pNA catalytic efficiency (k_{cat}/K_m) ratio for the I491W FAAH mutant (3670/240 =

15.3) was 90-fold greater than the k_{cat}/K_m ratio for the I491Y mutant (140/820 = 0.17). The differences in substrate selectivity displayed by the various I491 mutants are noteworthy given that they resulted from a limited number of mutations in a single residue of FAAH and without the aid of a three-dimensional structure. Considering that more than 80 AS enzymes are present in living organisms, many of which have evolved diverse and highly specialized substrate selectivities (*1*, *30*−*34*, *39*, *40*), this enzyme family appears particularly well suited for the design and in vitro evolution of amidases possessing novel and/or tailored specificities.

ACKNOWLEDGMENT

We thank Jiang Wu for performing tandem MS experiments and for providing general MS assistance and advice.

REFERENCES

1. Cravatt, B. F., Giang, D. K., Mayfield, S. P., Boger, D. L., Lerner, R. A., and Gilula, N. B. (1996) *Nature 384*, 83−7.
2. Giang, D. K., and Cravatt, B. F. (1997) *Proc. Natl. Acad. Sci. U.S.A. 94*, 2238−42.
3. Deutsch, D. G., and Chin, S. A. (1993) *Biochem. Pharmacol. 46*, 791−6.
4. Maurelli, S., Bisogno, T., De Petrocellis, L., Di Luccia, A., Marino, G., and Di Marzo, V. (1995) *FEBS Lett. 377*, 82−6.
5. Desarnaud, F., Cadas, H., and Piomelli, D. (1995) *J. Biol. Chem. 270*, 6030−5.
6. Ueda, N., Kurahashi, Y., Yamamoto, S., and Tokunaga, T. (1995) *J. Biol. Chem. 270*, 23823−7.
7. Devane, W. A., Hanus, L., Breuer, A., Pertwee, R. G., Stevenson, L. A., Griffin, G., Gibson, D., Mandelbaum, A., Etinger, A., and Mechoulam, R. (1992) *Science 258*, 1946−9.
8. Cravatt, B. F., Prospero-Garcia, O., Siuzdak, G., Gilula, N. B., Henriksen, S. J., Boger, D. L., and Lerner, R. A. (1995) *Science 268*, 1506−9.
9. Cravatt, B. F., Lerner, R. A., and Boger, D. L. (1996) *J. Am. Chem. Soc. 118*, 580−590.
10. Felder, C. C., Briley, E. M., Axelrod, J., Simpson, J. T., Mackie, K., and Devane, W. A. (1993) *Proc. Natl. Acad. Sci. U.S.A. 90*, 7656−60.
11. Vogel, Z., Barg, J., Levy, R., Saya, D., Heldman, E., and Mechoulam, R. (1993) *J. Neurochem. 61*, 352−5.
12. Crawley, J. N., Corwin, R. L., Robinson, J. K., Felder, C. C., Devane, W. A., and Axelrod, J. (1993) *Pharmacol. Biochem. Behav. 46*, 967−72.
13. Smith, P. B., Compton, D. R., Welch, S. P., Razdan, R. K., Mechoulam, R., and Martin, B. R. (1994) *J. Pharmacol. Exp. Ther. 270*, 219−27.
14. Fride, E., and Mechoulam, R. (1993) *Eur. J. Pharmacol. 231*, 313−4.
15. Lerner, R. A., Siuzdak, G., Prospero-Garcia, O., Henriksen, S. J., Boger, D. L., and Cravatt, B. F. (1994) *Proc. Natl. Acad. Sci. U.S.A. 91*, 9505−8.
16. Basile, A. S., Hanus, L., and Mendelson, W. B. (1999) *Neuroreport 10*, 947−51.
17. Hedlund, P. B., Carson, M. J., Sutcliffe, J. G., and Thomas, E. A. (1999) *Biochem. Pharmacol. 58*, 1807−13.
18. Thomas, E. A., Carson, M. J., Neal, M. J., and Sutcliffe, J. G. (1997) *Proc. Natl. Acad. Sci. U.S.A. 94*, 14115−9.
19. Huidobro-Toro, J. P., and Harris, R. A. (1996) *Proc. Natl. Acad. Sci. U.S.A. 93*, 8078−82.
20. Boger, D. L., Patterson, J. E., and Jin, Q. (1998) *Proc. Natl. Acad. Sci. U.S.A. 95*, 4102−7.
21. Lees, G., Edwards, M. D., Hassoni, A. A., Ganellin, C. R., and Galanakis, D. (1998) *Br. J. Pharmacol. 124*, 873−82.
22. Wakamatsu, K., Masaki, T., Itoh, F., Kondo, K., and Sudo, K. (1990) *Biochem. Biophys. Res. Commun. 168*, 423−9.
23. Cadas, H., di Tomaso, E., and Piomelli, D. (1997) *J. Neurosci. 17*, 1226−42.
24. Sugiura, T., Kondo, S., Sukagawa, A., Tonegawa, T., Nakane, S., Yamashita, A., and Waku, K. (1996) *Biochem. Biophys. Res. Commun. 218*, 113−7.
25. Arafat, E. S., Trimble, J. W., Andersen, R. N., Dass, C., and Desiderio, D. M. (1989) *Life Sci. 45*, 1679−87.
26. Chebrou, H., Bigey, F., Arnaud, A., and Galzy, P. (1996) *Biochim. Biophys. Acta 1298*, 285−93.
27. Sako, Y., Nomura, N., Uchida, A., Ishida, Y., Morii, H., Koga, Y., Hoaki, T., and Maruyama, T. (1996) *Int. J. Syst. Bacteriol. 46*, 1070−7.
28. Mayaux, J. F., Cerebelaud, E., Soubrier, F., Faucher, D., and Petre, D. (1990) *J. Bacteriol. 172*, 6764−73.
29. Kobayashi, M., Komeda, H., Nagasawa, T., Nishiyama, M., Horinouchi, S., Beppu, T., Yamada, H., and Shimizu, S. (1993) *Eur. J. Biochem. 217*, 327−36.
30. Boshoff, H. I., and Mizrahi, V. (1998) *J. Bacteriol. 180*, 5809−14.
31. Hashimoto, Y., Nishiyama, M., Ikehata, O., Horinouchi, S., and Beppu, T. (1991) *Biochim. Biophys. Acta 1088*, 225−33.
32. Kim, Y. S., and Kang, S. W. (1994) *J. Biol. Chem. 269*, 8014−21.
33. Curnow, A. W., Hong, K., Yuan, R., Kim, S., Martins, O., Winkler, W., Henkin, T. M., and Soll, D. (1997) *Proc. Natl. Acad. Sci. U.S.A. 94*, 11819−26.
34. Gomi, K., Kitamoto, K., and Kumagai, C. (1991) *Gene 108*, 91−8.
35. Ettinger, R. A., and DeLuca, H. F. (1995) *Arch. Biochem. Biophys. 316*, 14−19.
36. Patricelli, M. P., Lovato, M. A., and Cravatt, B. F. (1999) *Biochemistry 38*, 9804−12.
37. Patricelli, M. P., and Cravatt, B. F. (1999) *Biochemistry 38*, 14125−30.
38. Patricelli, M. P., and Cravatt, B. F. (2000) *J. Biol. Chem. 275*, 19177−84.
39. Thomashow, M. F., Hugly, S., Buchholz, W. G., and Thomashow, L. S. (1986) *Science 231*, 616−8.
40. Okada, H., Negoro, S., Kimura, H., and Nakamura, S. (1983) *Nature 306*, 203−6.
41. De Muynck, H., Madder, A., Farcy, N., De Clercq, P. J., Perez-Payan, M. N., and Ohberg, L. M. (2000) *Angew. Chem., Int. Ed. Engl. 39*, 145−148.
42. Koeller, K. M., and Wong, C. H. (2001) *Nature 409*, 232−240.
43. Patricelli, M. P., Lashuel, H. A., Giang, D. K., Kelly, J. W., and Cravatt, B. F. (1998) *Biochemistry 37*, 15177−87.
44. Deutsch, D. G., Omeir, R., Arreaza, G., Salehani, D., Prestwich, G. D., Huang, Z., and Howlett, A. (1997) *Biochem. Pharmacol. 53*, 255−60.
45. Keana, J. F. W., and Cai, S. X. (1990) *J. Org. Chem. 55*, 3640−3647.
46. Lang, W., Qin, C., Lin, S., Khanolkar, A. D., Goutopoulos, A., Fan, P., Abouzid, K., Meng, Z., Biegel, D., and Makriyannis, A. (1999) *J. Med. Chem. 42*, 1682.
47. Boger, D. L., Henriksen, S. J., and Cravatt, B. F. (1998) *Curr. Pharm. Des. 4*, 303−14.
48. Boger, D. L., Sato, H., Lerner, A. E., Austin, B. J., Patterson, J. E., Patricelli, M. P., and Cravatt, B. F. (1999) *Bioorg. Med. Chem. Lett. 9*, 265−70.
49. Boger, D. L., Sato, H., Lerner, A. E., Hedrick, M. P., Fecik, R. A., Miyauchi, H., Wilkie, G. D., Austin, B. J., Patricelli, M. P., and Cravatt, B. F. (2000) *Proc. Natl. Acad. Sci. U.S.A. 97*, 5044−9.
50. Dorman, G., and Prestwich, G. D. (1994) *Biochemistry 33*, 5661−73.
51. Rheinnecker, M., Eder, J., Pandey, P. S., and Fersht, A. R. (1994) *Biochemistry 33*, 221−5.
52. Rheinnecker, M., Baker, G., Eder, J., and Fersht, A. R. (1993) *Biochemistry 32*, 1199−203.
53. Craik, C. S., Largman, C., Fletcher, T., Roczniak, S., Barr, P. J., Fletterick, R., and Rutter, W. J. (1985) *Science 228*, 291−7.

BI002578R